

Trend of Santonian (Late Cretaceous) atmospheric CO₂ and global mean land surface temperature: Evidence from plant fossils

WAN ChuanBiao¹, WANG DeHai², ZHU ZhanPing² & QUAN Cheng^{3*}

¹Exploration and Development Research Institute, Daqing Oilfield Company Ltd., Daqing 163712, China;

²College of Geosciences, Jilin University, Changchun 130061, China;

³Key Laboratory for Evolution of Past Life and Environment in Northeast China, MOE, Jilin University, Changchun 130026, China

Received May 25, 2010; accepted November 17, 2010; published online August 5, 2011

Quantitative reconstructions of atmospheric CO₂ by using terrestrial and marine records are critical for understanding the so-called “greenhouse” conditions in the Cretaceous, but data from terrestrial plants for several stages of this period remain quite limited. Using the stomatal index (SI) technique, here we estimate the Santonian (Late Cretaceous) CO₂ contents based on a sequence of fossil cuticles of *Ginkgo adiantoides* (Ung.) Heer from three beds of the Yong’ancun Formation in Jiayin, Heilongjiang Province, northeastern China. By the regress function, SIs of *Ginkgo* fossils reveal a pronounced CO₂ reduction from the early to late Santonian (~661 and ~565 ppm, respectively). The relatively high CO₂ levels provide additional evidence for paleoclimatic warmth in this interval. Moreover, available paleobotanical data illustrate a decline trend of CO₂ contents throughout the Late Cretaceous, punctuated by several fluctuations in particular episodes with different magnitudes. The CO₂ contents shifted notably in the late Cenomanian, Turonian, early Santonian, late Campanian, and probably latest Maastrichtian. Furthermore, a comprehensive study based on CO₂ data shows that the global mean land surface temperature (GMLST) fluctuated several times accordingly. The change ratios of GMLST (ΔT) increased from ~3°C in late Cenomanian to ~4.7°C in mid Turonian, and then dramatically reduced to ~2.2°C in mid Coniacian. From the Santonian onward, it appears that the temperature gradually decreased with a few minor fluctuations.

Santonian, Late Cretaceous, global mean land surface temperature, stomatal index, Yong’ancun Formation, Jiayin

Citation: Wan C B, Wang D H, Zhu Z P, et al. Trend of Santonian (Late Cretaceous) atmospheric CO₂ and global mean land surface temperature: Evidence from plant fossils. *Sci China Earth Sci*, 2011, 54: 1338–1345, doi: 10.1007/s11430-011-4267-1

In geological history, the Cretaceous represents one of the most remarkable periods for several critical geological events occurred, such as the Oceanic Anoxic Events [1] and K-T event [2]. These events triggered environmental changes and had profound impacts on the biosphere [3–5]. Among several factors, atmospheric carbon dioxide (CO₂) contributed substantially to the environmental changes [3, 5]. Many biological events in this interval have been linked to the trend of CO₂, including the radiation and diversifica-

tion of angiosperms [3, 6]. However, the data of Cretaceous CO₂ levels are derived mainly from geochemical models or proxies with different timescale resolution [7–10]. The quantitative reconstructions of the Cretaceous CO₂ in separate stages based on paleobotanical data [11–16] are far from complete.

Plants employ various adaptation strategies to help them survive in different areas and environments. Almost all morphological features, including the epidermis and the overlying cuticle, vary according to particular environmental conditions under which the plants grow [17–19]. The cuticle, with the stomata in it, is the interface between plant

*Corresponding author (email: quan@jlu.edu.cn)

interior and surrounding environment. On the one hand, it acts as a barrier that limits water loss from epidermal cells [20]; on the other hand, the plant controls stomatal movements to regulate the uptake of CO₂ from the ambient atmosphere and the evaporation of water out of the plant [21]. These and other physiological responses, in a given environmental condition, have to be based on a most economic structure by which the plant can survive at an optimal efficiency on obtaining basic resources [22], such as CO₂, light intensity, and nutrients.

The relationship between stomata and atmospheric CO₂ has long been recognized. Investigations on extant plants and fossil records, as well as from controlled experiments, have shown that stomatal parameters are inversely related to CO₂ content [18, 19, 23, 24]. Two parameters are usually involved, stomatal density (SD, number of stomata per unit leaf area) and stomatal index (SI, percentage of stomata on the epidermis to the total cell number). But the SD varies considerably with the change of environmental factors, such as light intensity, temperature, and water stress. The SI, in contrast, is sensitive only to factors affecting cell initiation, of which CO₂ appears to be one [25]. Thus, for a given species, even if SD and SI show similar responses, SI yields more accurate estimates of CO₂ content [18, 19, 23, 25]. And among the taxa used in paleo-CO₂ reconstruction, conifers and parallel-veined gymnosperms are favorite ones, because their stomata are initiated regularly in certain areas [12, 18, 26, 27].

Here we report some new data on CO₂ contents during the Santonian (Late Cretaceous) derived from SIs of *Ginkgo adiantoides* (Ung.) Heer. The present and our previous studies in Jiayin [14] demonstrate that CO₂ levels gradually declined during the Santonian to Campanian. Furthermore, the trend of Late Cretaceous atmospheric CO₂ and global mean land surface temperature are discussed based on available paleobotanical CO₂ estimates of separate stages. These results therefore add new elements to the atmospheric CO₂ and paleoclimate reconstructions of the Late Cretaceous.

1 Materials and methods

1.1 Materials

The *Ginkgo* fossils were collected from the Nanshan section of the Late Cretaceous Yong'ancun Formation in 2009 and 2010 (Figures 1 and 2). This plant-bearing formation represents a shallow lacustrine and fluvial succession, consisting of grey mudstone, green-grey siltstone, and yellow-green sandstone [28]. It yields fossils of conchostracans, dinosaur footprints, fishes, and plants [28, 29]. Recent studies based on palynological data and stratigraphical correlation suggest that this formation is predominantly of Santonian age [29, 30].

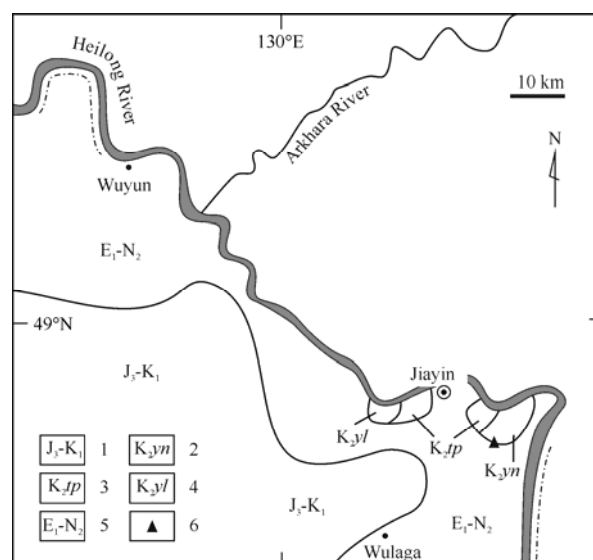


Figure 1 Geological scheme of the Jiayin basin and geographical position of *Ginkgo* fossil locality in Jiayin, Heilongjiang, NE China. 1, Upper Jurassic to Lower Cretaceous; 2, Yong'ancun Formation; 3, Taipinglinchang Formation; 4, Yuliangzi Formation; 5, lower Paleogene to middle Neogene; 6, Nanshan section of Yong'ancun Formation.

The fossil plants of the Yong'ancun Formation come from fluvial accumulations of the upper delta plains, which appears to be related to freshwater environments and have no evidence of stress conditions produced by brackish-water environments near the fossil-bearing beds [30]. The plant assemblage is interpreted as the remains of an open vegetation developed in conditions of relatively high humidity [29].

1.2 Cuticle preparation, counting data, and paleotemperature analysis

A total of 31 leaves of *G. adiantoides* with well-preserved cuticles were collected from three beds of the Yong'ancun Formation, but most of them are fragmentary (Figure 2). The stomatal index measurements were performed on at least eight leaves per bed, more than the minimum number that ensures the fidelity of mean SI in *Ginkgo* (five leaves [18]). The cuticles are prepared and counted following our previous study [14]. In total, the counts were carried out on 94 fragments of 31 specimens. The statistic stomatal values reported here are averages of all measurements for each leaf per bed. All experimental works were carried out in the Key Laboratory for Evolution of Past Life and Environment in Northeast China, MOE, Jilin University, and the fossil specimens and cuticle preparations are kept there. The photographic instruments are JSM-6700F for SEM and Olympus DP12 for LM.

The stomatal index is calculated as: SI (%) = [SD/(SD+ED)]×100, where an ED = non-stomatal epidermal cell density (subsidiary cells and ordinary epidermal cells). The

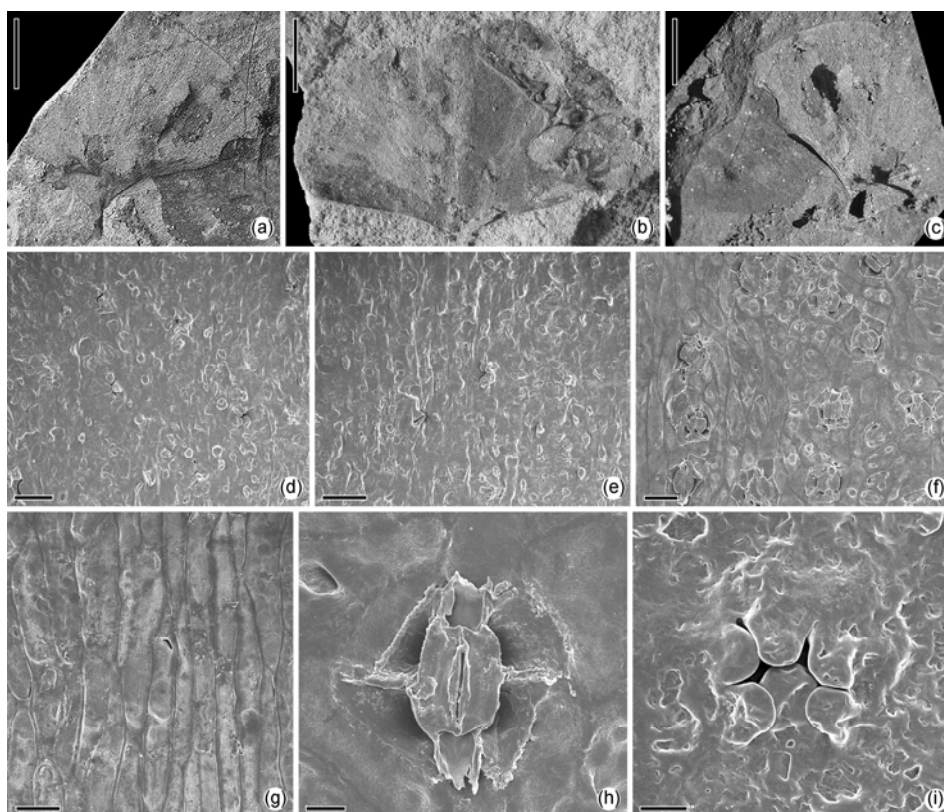


Figure 2 Fossil leaves and abaxial cuticle of *Ginkgo adiantoides* from the Yong'ancun Formation. (a)–(c) Gross morphology of leaves, bars = 1 cm; (d) outer view of stomatal zone, bar = 50 μm ; (e) outer view of coastal zone (middle), bar = 50 μm ; (f) inner view of stomatal zone, bar = 40 μm ; (g) inner view of coastal zone, bar = 20 μm ; (h) inner view of the stoma, bar = 10 μm ; (i) outer view of the stoma, bar = 10 μm .

Santonian atmospheric CO_2 contents are reconstructed from fossil *Ginkgo* cuticle SI by using the inverse regression function (RF) [31]:

$$\text{paleo-}\text{CO}_2 = \frac{(415 \times \text{SI} - 1961) \times 2000}{3337 \times \text{SI} - 20000}. \quad (1)$$

This formulation was derived from herbarium collections and controlled experiments of extant *Ginkgo biloba* L. leaves [31]. It can be used for the present Santonian material (*G. adiantoides*) owing to the extreme similarity in both ecological and anatomical features of these two forms [32–34].

To assess the results of this RF procedure, an alternative stomatal-based CO_2 method, nearest living equivalent (NLE), is used. An NLE is a modern taxon that has a comparable ecological setting and/or structural similarity to its fossil counterpart, and it is assumed that a stomatal ratio (SR, the ratio of the stomatal index of a modern NLE species to its fossil counterpart) of 1 is equal to 300 ppm (Recent standardization) or 600 ppm (Carboniferous standardization) [35]. The Recent and Carboniferous standardizations are regarded respectively as the broad minimum and maximum estimates of paleo- CO_2 [35]. However, we supposed that the Recent Standardization is more suitable than the Carboniferous one for the present material because the similarity in morphological, anatomical, and ecological features

[32–34], and relatively short geological span between these two *Ginkgo* species.

For tracking CO_2 fluctuations on a larger scale, the NLE-based Santonian ratio of CO_2 values (R_{CO_2} , the ratio of the mass of CO_2 in the atmosphere in the past to that of pre-industrial level) of present study are also calculated. The NLE of fossil *Ginkgo adiantoides* is obviously *G. biloba*, yielding an SI of 12.1 on average [18].

Based on obtained paleobotanical data from Jiayin and some others' results, the global mean land surface temperature (GMLST) is also calculated. The extent of associated climate change was calculated with the formula given by Kothavala et al. [36]:

$$\Delta T = 4.0 \times \ln(R_{\text{CO}_2}), \quad (2)$$

where ΔT is the change ratio in mean global surface temperature. This model-based formulation assumes a greenhouse-gas relation between CO_2 and temperature [36].

2 Results and comparisons

2.1 Stomatal index and paleo- CO_2

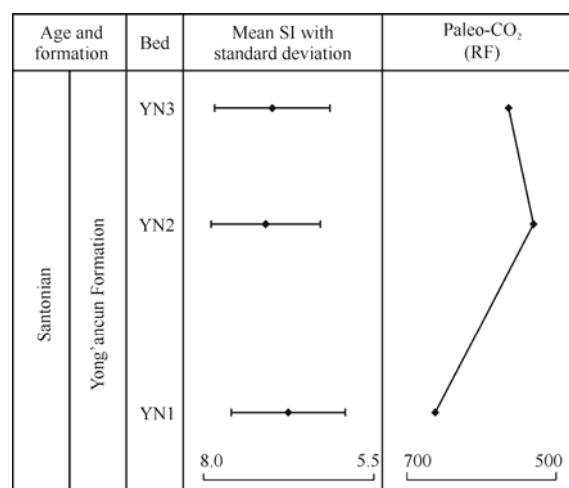
The statistical stomatal indices of all specimens are summarized in Table 1, and the average value per bed is plotted on

Table 1 Measurements of stomatal parameters of *Ginkgo adiantoides* from the Yong'ancun Formation of Jiayin

Beds	Specimens	ED (mean)	SI (%)	Mean SI (%)	Std of SI
YN3	YN09023	462.14	6.71	6.99	0.79
	YN09024	446.54	6.78		
	YN09026	438.21	7.30		
	YN09027	425.53	6.77		
	YN09028	472.60	6.95		
	YN09030	482.18	6.22		
	YN09031	458.59	6.76		
	YN09042	433.88	7.22		
	YN09046	435.48	7.37		
	YN09049	453.37	6.37		
	YN09051	451.43	7.73		
	YN09052	424.58	6.57		
	YN09055	456.55	7.72		
YN09056	455.31	7.14			
YN09058	499.64	7.22			
YN2	YN09017	455.54	6.81	7.11	0.65
	YN09018	459.36	7.47		
	YN10005	633.92	5.71		
	YN10018	459.17	7.11		
	YN10019	445.84	7.53		
	YN10020	417.88	6.97		
YN1	YN10023	438.64	7.60	6.76	0.83
	YN10024	484.17	7.69		
	YN09001	485.75	6.57		
	YN09002	547.37	7.27		
	YN09003	535.44	6.66		
	YN09006	567.77	6.04		
	YN09008	441.37	6.17		
	YN09014	517.09	6.57		
	YN09015	539.70	7.67		
YN09016	552.71	7.12			

Figure 3. The SI value of each fossil *G. adiantoides* is significantly lower than the value of extant *G. biloba* (about 12.1 on average [18]) (Table 1), indicating a much higher atmospheric CO₂ content in the Santonian. RF-based CO₂ estimates from the SI analyses vary from ~661 ppm in the early Santonian to ~531 ppm in the middle and ~565 ppm in the late Santonian (Table 2), which is 150–280 ppm higher than the present day (~380 ppm [37]).

From stomatal index measurements (Table 2), we next calculated the stomatal ratios (SR, the ratio of the SI of the nearest living ecological equivalent to that of the fossil). These were then converted to R_{CO_2} values following the standard procedure of NLE method [35]. Calculated in this way, the NLE-based CO₂ reconstructions closely agree with the RF-based result (Table 2, Figure 4(a)). The CO₂ content declined from the early Santonian (~503 ppm, bed YN1, recent standardization) to the minimum in the mid Santonian (~478 ppm, bed YN2), and then rebounded slightly in the late Santonian (~486 ppm, bed YN3) (Table 2). As shown in Figure 4(a), it is apparent that RF-results fall in the range of NLE ones. Moreover, despite the slightly higher estimates of RF method (~97 ppm on average), the two

**Figure 3** SIs of *G. adiantoides* and paleo-CO₂ estimates for separate beds of the Yong'ancun Formation (error bars show standard deviation).**Table 2** Inferred Santonian CO₂ based on *Ginkgo* cuticles^{a)}

Bed	YN1	YN2	YN3
Mean SI (%)	6.76	7.11	6.99
Standard deviation	0.83	0.65	0.79
RF-CO ₂ (ppm)	660.82	530.58	565.19
R_{CO_2}	1.68	1.59	1.62
R.S. (ppm)*	502.90	477.89	486.26
Sigma-1 (ppm)	452.61	430.10	437.63
C.S. (ppm)*	1005.80	955.79	972.52
Sigma +1 (ppm)	1106.38	1051.36	1069.77

a) * R.S., Recent standardization; C.S., Carboniferous standardization.

sets of stomata-based results suggest a modest decrease of CO₂ throughout the Santonian (Table 2, Figure 4(a)).

2.2 Comparison to geochemical data

To date, few paleobotanical data of Santonian CO₂ have been published, so the new data are compared to the estimates from geochemical proxies and predictions from geochemical models of the long-term global carbon cycle.

The present data of Santonian CO₂ content are most compatible with the levels estimated by GEOCARB II of Berner [7]. Although the RF-results of present study show a higher value than that of GEOCARB II in the early Santonian (about 90 ppm), the late Santonian ones of both studies are almost the same (Figure 4(a)). Moreover, the NLE-results (Recent standardization) are also closely comparable to GEOCARB II (Figure 4(a)). GEOCARB III [8] predicts a Santonian CO₂ value of about 1270 ppm, which is much higher than the present study although the present values (both RF- and NLE-based) lie in the overall range of GEOCARB II and III. Some authors [12, 16] have argued, although as a more refined model, GEOCARB III produces higher concentrations in Cretaceous CO₂ than that of GEOCARB II, and GEOCARB II might be better supported

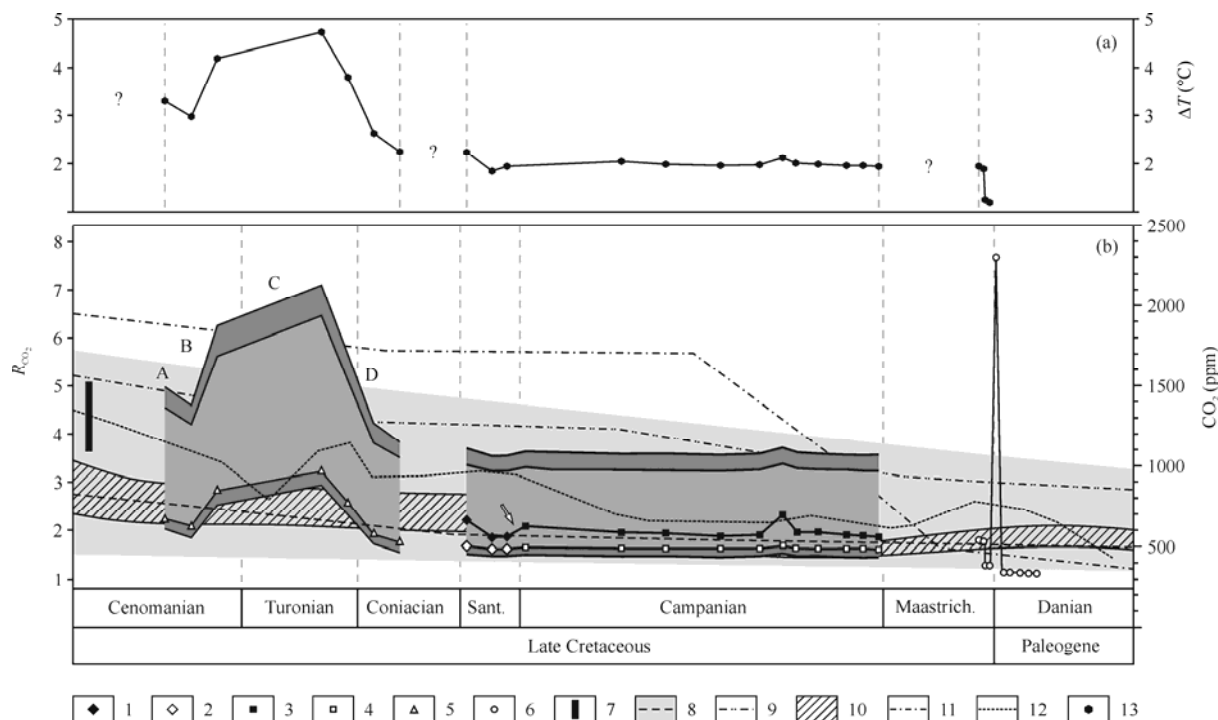


Figure 4 Atmospheric CO₂ (a) and global mean land surface temperature (b) trends in the Late Cretaceous. 1, RF-results of the present study; 2, NLE-results of the present study; 3, RF-based Campanian results from Quan et al. [14]; 4, NLE-based Campanian results from Quan et al. [14]; 5, recalibrated results (NLE) from Retallack [15]; 6, RF-based Maastrichtian results from Beerling et al. [11]; 7, Cenomanian result from isotope of fossil bryophytes [44]; 8, GEOCARB II with error range [7]; 9, GEOCARB III [8]; 10, box model of Wallmann [39]; 11, geochemical values from Ekart et al. [9]; 12, biogeochemical carbon cycle model from Tajika [10]; 13, change ratios of global mean land surface temperature (ΔT).

by independent paleobotanical data. It appears that this may also be the case for the Late Cretaceous Jiayin materials.

Ekart et al. [9] reported a CO₂ content by a paleobarometer derived from carbon isotope record of pedogenic carbonate, which implies the CO₂ levels lowered through the Cretaceous, dropping to less than 1000 ppm prior to the Cretaceous-Tertiary boundary. The Santonian CO₂ value of Ekart et al. [9] is about 1270 (± 500) ppm. The present result is within the ranges proposed by geochemical values by considering its error bars (Figure 4(a)). It is noteworthy that the paleosol-derived CO₂ estimates are mostly much higher than the paleobotanical ones, which might be caused by the different sensitivities of different proxies [18, 38].

The carbon cycle and climate change during the Cretaceous are also reconstructed by using a carbon cycle model by Tajika [10]. This model takes into account the effects of both long-term (e.g. organic carbon burial rates) and short-term (e.g. the enhanced magma eruption) biogeochemical processes on atmospheric CO₂, both of which are thought to influence the carbon cycle during the Cretaceous [10]. This model predicts a notable CO₂ decline from the Santonian to Campanian (~970 – ~650 ppm). For the Jiayin data, by comparison, although a decline trend of CO₂ is recognized, the magnitude is of narrow range (Figure 4(a)).

More recently, Wallmann [39] reported his box model for the Cretaceous to Cenozoic global carbon-calcium-strontium cycle. This model accounts for carbon masses in

ocean and atmosphere, in carbonate, and in particulate organic carbon (POC). According to Wallmann [39], the high Ca concentrations during the Cretaceous indicate the decline of atmospheric CO₂, since the negative feed-back provided by POC burial, which is coupled to CO₂-dependent weathering rates. For the Santonian atmospheric CO₂, the present result is in agreement with Wallmann's model; both show a downward trend (Figure 4(a)). However, the present result demonstrates that the CO₂ declined more rapidly from the early to mid and late Santonian (661, 531 and 565 ppm, respectively; RF). This difference is possibly caused by the different resolutions of these two studies. In addition, based on geochemical data, Wallmann [39] and other authors [40] inferred the Santonian as a climate optimum period, and probably caused by enhanced volcanic or tectonic activity by which greenhouse gases released, such as CO₂ and possibly methane [41]. The similar conditions might be in the Jiayin area of Santonian age because tuffaceous mud- and siltstone can be found in several beds of the Yong'ancun Formation [28].

3 Discussion

3.1 Late Cretaceous CO₂

Haworth et al. [12] published long time-scaled mid-Cretaceous CO₂ reconstruction using the NLE method based on

SIs of *Pseudofrenelopsis*. Their results show relatively low and only slight varying CO₂ over the Hauterivian-Albian interval. Two studies have also been undertaken based on *Ginkgo coriacea* Florin from the early-middle Early Cretaceous Huolinhe Formation of northeastern China [16, 42]. For the Late Cretaceous atmospheric CO₂, however, a few paleobotanical data have been published. The Late Cretaceous is the essential transition period during which biosphere evolved from Mesozoic to Cenozoic, and several profound events occurred in this period, including environment changes and the rise of angiosperms [3, 4, 43]. Here we combine the available paleobotanical data to discuss the trend of Late Cretaceous CO₂.

Fletcher et al. [44] developed a novel CO₂ proxy based on the stable carbon isotope composition ($\delta^{13}\text{C}$) of astomatous land plants. The analysis on fossil liverworts, from Alexander Island of Antarctica, yields an early Cenomanian CO₂ content of 1000–1400 ppm. Their value consist of independent proxy data and long-term carbon cycle models [44]. And this value is also well supported by recalibrated stomatal data of conifers and ginkgoals from the Southern Hemisphere [13].

Retallack [15], by gathering data from the extant *Ginkgo* and four fossil relatives, first published stomata-based CO₂ reconstruction back to 300 million years ago. The general CO₂ pattern is correlated well with the long-term temperature pattern established by oxygen isotope ratios derived from marine fossils. This study is of importance since the record is based on the stomatal indices of ginkgoalean affinities, by which it minimizes the potential influences such as humidity, temperature, and light irradiation. However, some of the data suffer a large variability of stomatal index because of the small sample size (commonly less than 4) and by the use of an inappropriate transfer function [18]. Here we re-calculated the Retallack's original ginkgoalean data of Late Cretaceous since few paleobotanical data have been reported from this interval. The NLE method is used here rather than RF. First of all, the stomatal responses to CO₂ are species-specific [25]. Retallack's species include *Ginkgo sibirica* Heer, *G. pilifera* Samylin, and *G. transsenonicus* Krassilov; the regression function derived from extant *G. biloba* consequently is impracticable here. Secondly, the morphological and anatomical features of some species appear varying significantly, such as *G. pilifera* and *G. transsenonicus*, which yield amphistomatous cuticles [14].

The re-calibration illustrates a series of dramatic changes during the mid Cenomanian to mid Coniacian (at a resolution of about 1 million years, Figure 4(a)). We subdivide it into four stages (marked respectively as A–D in Figure 4(a)). In stage A, atmospheric CO₂ declines from ~680 to ~630 ppm, and then rebounds up to 850 ppm in stage B. In stage C, the level rises continuously to 971 ppm on the basis of stage B, but in a lower trend. A sharp decline occurs in stage D, falling from ~970 to ~520 ppm (Figure 4(a)). As a whole, although with drastic fluctuations as illustrated in

Figure 4(a), the recalibrated result shows an overall decline from the mid Cenomanian (~680 ppm) to mid Coniacian (~520 ppm). Besides, the fluctuation pattern of the recalibrated data matches well with Tajika [10] in the mid Turonian to early Coniacian. However, it is noteworthy that the late Cenomanian to mid Turonian CO₂ is opposite to those of geochemical data, which show a decline in trend (Figure 4(a)). Therefore more detailed evidence is needed to confirm the CO₂ levels of this interval.

For the late Coniacian, there are no paleobotanical data available, but it appears there is a slightly decline trend in the interval (Figure 4(a)).

Ginkgo fossils from Jiayin provided solid evidence for the Santonian to Campanian CO₂ as showing in the present and previous studies [14] (Figure 4(a)). Our paleobotanical data demonstrate a considerable decrease with magnitude of ~100 ppm (RF-based). This is not recognized by other geochemical results, probably due to the different resolutions of the two approaches.

For the mid Santonian to early Campanian, our data show a relative rapid rise, from ~531 to ~620 ppm (arrow in Figure 4(a)). However, this rapid rise needs to be further confirmed because the earliest Campanian CO₂ was reconstructed based only on one fossil *Ginkgo* specimen [14]. From this interval onward, the CO₂ levels show a gradual decrease from ~580 to 550 ppm with the exception of a short-time fluctuation (up to ~690 ppm) in the late Campanian. After the late Campanian CO₂ fluctuation, it appears that no striking changes in paleo-CO₂ occurred during the Maastrichtian, and the CO₂ level gradually decreased to 530 ppm until the K-T event [11] (Figure 4(a)).

In summary, geochemical studies predict that atmospheric CO₂ levels underwent a long-term decline through the Late Cretaceous [7–10, 39], ranging from about 1975 to 450 ppm (Figure 4(a)). By comparison, the paleobotanical results also indicate a decline trend in CO₂ content, but several fluctuations are recognized, as shown in Figure 4(a).

3.2 Global mean land surface temperature

The variation of global mean land surface temperature (GMLST) depends on the sensitivity of the climate system to changes in greenhouse gas concentrations, such as carbon dioxide and methane [45]. But because of the short residence time of CH₄ for its easy oxidability, the CO₂ pertains more directly to the long-term global land surface temperature. This relationship has long been recognized [37]. The generally accepted range for the equilibrium means temperature change in response to a doubling of the atmospheric CO₂ content [45].

Geochemical data show that warmer conditions prevailed during much of the Cretaceous with exception of brief episodes of cooling (~3 Ma), such as mid-Cenomanian, mid-Turonian, and Maastrichtian [46]. Retallack [15] pro-

vided a broad picture of CO₂ variation throughout the Phanerozoic. His results are largely consistent with the predictions of carbon mass-balance models and with reconstructions inferred from marine geochemical data [17], showing that warming trends are accompanied by increasing CO₂ levels, whereas cooler periods are accompanied by reduced CO₂. However, these paleobotanical records are incomplete; some gaps still need to be filled. Here we compile the present and published stomata-based CO₂ data to discuss GMLST during the Late Cretaceous.

Applying the paleo-CO₂ estimations from *Ginkgo* and affinities of separate stages into the transfer function shown as formulation (2) (see Materials and methods), we plotted the change ratios of GMLST (ΔT) from present day values in Figure 4(b). It illustrates that during the mid Cenomanian to mid Coniacian the temperature fluctuated several times, ranging from ~2.2–4.7°C (Figure 4(b), Table 3). From the Santonian onward, although the punctuations exist (one decline in the mid Santonian and one increase in late Campanian), the stomatal data broadly display a stepwise reduction in GMLST (Figure 4(b)). To the latest Maastrichtian, however, the stomatal data show an evident GMLST decline, suggesting a slight cooling from ~1.9 to 1.2°C (Figure 4(b), Table 3). This GMLST curve is largely in agreement with the stable carbon- and oxygen-isotopic patterns

based on hemipelagic carbonate facies from the Upper Cretaceous of Tibet, China by Li et al. [47], especially in the Santonian, Campanian, and Maastrichtian stages.

4 Conclusions

Paleobotanical data derived from fossil *G. adiantoides* of the Yong'ancun Formation suggest the Santonian CO₂ content declined from ~661 to ~565 ppm (RF). Our stomata-based CO₂ estimates (both RF and NLE methods) are most compatible with the GEOCARB II model. A relatively higher atmosphere CO₂ helps explain the environment of this stage.

Available paleobotanical data show a decrease trend of CO₂ level throughout the Late Cretaceous, punctuated by several fluctuations in particular episodes. The atmospheric CO₂ fluctuated notably in the late Cenomanian, Turonian, early Santonian, late Campanian, and probably latest Maastrichtian. All these episodes appear to be in certain critical geological intervals, but the ultimate mechanisms underlying the shift remain unknown from the present study.

In addition, the change ratios of CO₂-driven GMLST illustrate that the trend of temperature during the Late Cretaceous varies in a very similar way to that of carbon- and oxygen-isotopic records. To view the variation as a whole, ΔT increased from ~3°C in late Cenomanian to ~4.7°C in mid Turonian, and then dramatically reduced to ~2.2°C in mid Coniacian. From the Santonian onward, it appears that GMLST gradually declined with a few punctuations.

Table 3 Stomata-based R_{CO_2} and change ratios of global mean land surface temperature during the Late Cretaceous^{a)}

Stage	Age (Ma) or bed	Mean SI (%)	R_{CO_2}	ΔT (°C)
Maast.*	65.4	8.40	1.35	1.20
	65.5	8.30	1.37	1.24
	65.8	7.10	1.60	1.87
	65.9	7.00	1.62	1.93
Camp.	TP11	7.01	1.62	1.92
	TP10	6.98	1.62	1.94
	TP09	6.97	1.63	1.94
	TP08	6.92	1.64	1.97
	TP07	6.91	1.64	1.98
	TP06	6.70	1.69	2.10
	TP05	6.96	1.63	1.95
	TP04	6.98	1.62	1.94
	TP03	6.94	1.63	1.96
	TP02	6.93	1.63	1.97
	TP01	6.83	1.66	2.02
Sant.	YN3	6.99	1.62	1.93
	YN2	7.11	1.59	1.86
	YN1	6.76	1.68	2.07
Ceno.-Con.	87	6.5	1.74	2.22
	88	5.9	1.92	2.61
	89	4.4	2.58	3.78
	90	3.5	3.24	4.70
	94	4.0	2.83	4.16
	95	5.4	2.10	2.96
	96	5.0	2.27	3.27

a) *Assuming the K-T boundary = 65 Ma [11].

We are grateful to Prof. Sun B. N. and Dr. Xie S. P. (Lanzhou University) for helpful suggestions. Thanks go to the anonymous reviewers for constructive comments. This work was supported by the National Basic Research Program of China (Grant No. 2006CB701401), the National Natural Science Foundation of China (Grant No. 41002004), China Postdoctoral Science Foundation (Grant No. 20090451258), and the Fund of LPS, Nanjing Institute of Geology and Palaeontology, CAS (Grant No. 103107).

- 1 Wang C S, Hu X M, Sarti M, et al. Upper Cretaceous oceanic red beds in southern Tibet: A major change from anoxic to oxic, deep-sea environments. *Cretaceous Res*, 2005, 26: 21–32
- 2 Alvarez L W, Alvarez W, Asaro F, et al. Extraterrestrial cause for the Cretaceous-Tertiary extinction-experimental results and theoretical interpretation. *Science*, 1980, 208: 1095–1108
- 3 McElwain J, Willis K J, Lupia R. Cretaceous CO₂ decline and the radiation and diversification of angiosperms. In: Ehleringer J R, Cerling T E, Dearing M D, eds. *A History of Atmospheric CO₂ and its Effects on Plants, Animals, and Ecosystems*. Berlin: Springer-Verlag, 2005. 133–165
- 4 Davies A, Kemp A E S, Pike J. Late Cretaceous seasonal ocean variability from the Arctic. *Nature*, 2009, 460: 254–258
- 5 Royer D L, Berner R A, Park J. Climate sensitivity constrained by CO₂ concentrations over the past 420 million years. *Nature*, 2007, 446: 530–532
- 6 Heimhofer U, Hochuli P A, Burla S, et al. Timing of Early Cretaceous angiosperm diversification and possible links to major paleoenvironmental change. *Geology*, 2005, 33: 141–144
- 7 Berner R A. GEOCARB II: A revised model of atmospheric CO₂

- over Phanerozoic time. *Am J Sci*, 1994, 294: 56–91
- 8 Berner R A, Kothavala Z. GEOCARB III: A revised model of atmospheric CO₂ over Phanerozoic time. *Am J Sci*, 2001, 301: 182–204
 - 9 Ekart D D, Cerling T E, Montanez I P, et al. A 400 million year carbon isotope record of pedogenic carbonate: Implications for paleoatmospheric carbon dioxide. *Am J Sci*, 1999, 299: 805–827
 - 10 Tajika E. Carbon cycle and climate change during the Cretaceous inferred from a biogeochemical carbon cycle model. *Island Arc*, 1999, 8: 293–303
 - 11 Beerling D J, Lomax B H, Royer D L, et al. An atmospheric PCO₂ reconstruction across the Cretaceous-Tertiary boundary from leaf megafossils. *Proc Nat Acad Sci USA*, 2002, 99: 7836–7840
 - 12 Haworth M, Hesselbo S P, McElwain J C, et al. Mid-Cretaceous PCO₂ based on stomata of the extinct conifer *Pseudofrenelopsis* (Cheirolepidiaceae). *Geology*, 2005, 33: 749–752
 - 13 Passalia M G. Cretaceous PCO₂ estimation from stomatal frequency analysis of gymnosperm leaves of Patagonia, Argentina. *Palaeogeogr Palaeoclimatol Palaeoecol*, 2009, 273: 17–24
 - 14 Quan C, Sun C, Sun Y, et al. High resolution estimates of paleo-CO₂ levels through the Campanian (Late Cretaceous) based on *Ginkgo* cuticles. *Cretaceous Res*, 2009, 30: 424–428
 - 15 Retallack G J. A 300-million-year record of atmospheric carbon dioxide from fossil plant cuticles. *Nature*, 2001, 411: 287–290
 - 16 Sun B N, Xiao L, Xie S P, et al. Quantitative analysis of paleoatmospheric CO₂ level based on stomatal characters of fossil *Ginkgo* from Jurassic to Cretaceous in China. *Acta Geol Sin-Engl Ed*, 2007, 81: 931–939
 - 17 Kürschner W M. Leaf sensor for CO₂ in deep time. *Nature*, 2001, 411: 247–248
 - 18 Beerling D J, Royer D L. Fossil plants indicators of the Phanerozoic global carbon cycle. *Annu Rev Earth Planet Sci*, 2002, 30: 527–556
 - 19 Hetherington A M, Woodward F I. The role of stomata in sensing and driving environmental change. *Nature*, 2003, 424: 901–907
 - 20 Goodwin S M, Jenks M A. Plant cuticle function as a barrier to water loss. In: Matthew A, Jenks P M H, eds. *Plant Abiotic Stress*. Oxford: Blackwell Publishing, 2007. 14–36
 - 21 Pillitteri L J, Sloan D B, Bogenschutz N L, et al. Termination of asymmetric cell division and differentiation of stomata. *Nature*, 2007, 445: 501–505
 - 22 Wright I J, Reich P B, Westoby M, et al. The worldwide leaf economics spectrum. *Nature*, 2004, 428: 821–827
 - 23 Woodward F I. Stomatal numbers are sensitive to increases in CO₂ from pre-industrial levels. *Nature*, 1987, 327: 617–618
 - 24 Royer D L, Wing S, Beerling D J, et al. Paleobotanical evidence for near present day levels of atmospheric CO₂ during part of the Tertiary. *Science*, 2001, 292: 2310–2313
 - 25 Royer D L. Stomatal density and stomatal index as indicators of paleoatmospheric CO₂ concentration. *Rev Palaeobot Palynol*, 2001, 114: 1–28
 - 26 Sun B N, Yan D F, Xie S P, et al. *Stomata and Carbon Isotope of Fossil Plants and Their Applications* (in Chinese). Beijing: Science Press, 2009. 1–222
 - 27 Xie S, Sun B, Yan D, et al. Altitudinal variation in *Ginkgo* leaf characters: Clues to paleoelevation reconstruction. *Sci China Ser D-Earth Sci*, 2009, 52: 2040–2046
 - 28 Bureau of Geology and Mineral Resources of Heilongjiang Province. *Regional Geology of Heilongjiang Province* (in Chinese). Beijing: Geological Publishing House, 1993. 1–736
 - 29 Sun G, Akhmetiev M, Golovneva L, et al. Late Cretaceous plants from Jiayin along Heilongjiang River, Northeast China. *Forsch Inst Senck*, 2007, 258: 75–83
 - 30 Quan C, Sun G. Late Cretaceous aquatic angiosperms from Jiayin of Heilongjiang, Northeast China. *Acta Geol Sin-Engl Ed*, 2008, 82: 1133–1140
 - 31 Royer D L. Estimating latest Cretaceous and Tertiary atmospheric CO₂ from stomatal indices. In: Wing S L, Gingerich P D, Schmitz B, et al., eds. *Causes and Consequences of Globally Warm Climates in the Early Paleogene*. Boulder: The Geological Society of America, 2003. 79–93
 - 32 Tralau H. Evolutionary trends in the genus *Ginkgo*. *Lethaia*, 1968, 1: 63–101
 - 33 Royer D L, Hickey L J, Wing S L. Ecological conservatism in the “living fossil” *Ginkgo*. *Paleobiology*, 2003, 29: 84–104
 - 34 Quan C, Sun G, Zhou Z. A new Tertiary *Ginkgo* (Ginkgoaceae) from the Wuyun Formation of Jiayin, Heilongjiang, northeastern China and its palaeoenvironmental implications. *Am J Bot*, 2010, 97: 446–457
 - 35 McElwain J C. Do fossil plants signal palaeoatmospheric CO₂ concentration in the geological past? *Philos T R Soc B*, 1998, 353: 83–96
 - 36 Kothavala Z, Oglesby R J, Saltzman B. Sensitivity of equilibrium surface temperature of CCM3 to systematic changes in atmospheric CO₂. *Geophys Res Lett*, 1999, 26: 209–212
 - 37 Ding Z L, Duan X N, Ge Q S, et al. On the major proposals for carbon emission reduction and some related issues. *Sci China Earth Sci*, 2010, 53: 159–172
 - 38 Nordt L, Atchley S, Dworkin S I. Paleosol barometer indicates extreme fluctuations in atmospheric CO₂ across the Cretaceous-Tertiary boundary. *Geology*, 2002, 30: 703–706
 - 39 Wallmann K. Controls on the Cretaceous and Cenozoic evolution of seawater composition, atmospheric CO₂ and climate. *Geochim Cosmochim Acta*, 2001, 65: 3005–3025
 - 40 Forster A, Schouten S, Baas M, et al. Mid-Cretaceous (Albian-Santonian) sea surface temperature record of the tropical Atlantic Ocean. *Geology*, 2007, 35: 919–922
 - 41 Arthur M A, Dean W E, Schlanger S O. Variations in the global carbon cycle during the Cretaceous related to climate, volcanism, and changes in atmospheric CO₂. *Geophys Monogr*, 1985, 32: 504–29
 - 42 Chen L Q, Li C S, Chaloner W G, et al. Assessing the potential for the stomatal characters of extant and fossil *Ginkgo* leaves to signal atmospheric CO₂ change. *Am J Bot*, 2001, 88: 1309–1315
 - 43 Berner R A. The rise of plants and their effect on weathering and atmospheric. *Science*, 1997, 276: 544–546
 - 44 Fletcher B J, Beerling D J, Brentnall S J, et al. Fossil bryophytes as recorders of ancient CO₂ levels: Experimental evidence and a Cretaceous case study. *Global Biogeochem Cycles*, 2005, 19: 1–13
 - 45 Hegerl G C, Crowley T J, Hyde W T, et al. Climate sensitivity constrained by temperature reconstructions over the past seven centuries. *Nature*, 2006, 440: 1029–1032
 - 46 Royer D L. CO₂-forced climate thresholds during the Phanerozoic. *Geochim Cosmochim Acta*, 2006, 70: 5665–5675
 - 47 Li X, Jenkyns H C, Wang C, et al. Upper Cretaceous carbon- and oxygen-isotope stratigraphy of hemipelagic carbonate facies from southern Tibet, China. *J Geol Soc*, 2006, 163: 375–382